Environ. Sci. Technol. **1998**, *32,* 2909−2915

Quantification of Polymer Interactions in Bacterial Adhesion

BARBARA A. JUCKER, ALEXANDER J. B. ZEHNDER, AND HAUKE HARMS*

Swiss Federal Institute for Environmental Science and Technology (EAWAG) and Swiss Federal Institute of Technology (ETH), Überlandstrasse 133, CH-8600 Dübendorf, Switzerland

Adhesion of bacteria to solids is governed by van der Waals, electrostatic, and acid−base (hydrophobic) interactions, which are combined in an extended DLVO model (DLVO−AB) and by interactions of bacterial surface polymers with the solid surfaces. A method to calculate polymer interactions was not available yet, and their existence had been inferred only qualitatively from the deviation of the actual adhesion from DLVO−AB-based expectations. Here, we present attempts (i) to quantify polymer interactions from this deviation and (ii) to calculate them independently as the sum of repulsive and attractive contributions. Repulsion was assumed to result from the resistance of the polymer layer against compression. Its calculation was most sensitive to the packing density of the polymers in the cell envelope. Attraction was assumed to origin from polymer adsorption to the surface and was calculated on the basis of adsorption data of isolated surface polymers. Comparison of total interaction energy curves with adhesion of six Gram-negative bacteria to glass showed that the low adherence of five strains may have resulted from dominant polymer repulsion, i.e., hardly compressible cell envelopes hindered the bacteria to approach the energy minima resulting from DLVO−AB interactions. One strain adhered readily, possibly because polymer repulsion was low and polymer attraction and DLVO−AB forces dominated the overall interaction.

Introduction

Bacterial adhesion to solids as a crucial step in the initiation of biofilms has evoked the interest of biologists, physical chemists, material scientists, and civil engineers. Biofilms are the principle habitats of bacteria in nature as well as in the anthroposphere and harbor the majority of all microbial activities. Adhesion to solids also controls the mobility of bacteria in the subsurface and, thus, affects the bacteriological safety of drinking water resources. It is believed that adhesion of bacteria to solids is governed by long-ranging interactions and by immediate interactions between bacterial surface polymers and solid surfaces. The long-ranging electrostatic and van der Waals forces have been combined in the DLVO model of colloid stability (*1*). Later, this model has been extended by acid−base (hydrophobic) interactions, which account for the long-ranging effects of electron acceptor and donor groups on the surface on the structure of the adjacent water (*2*). This extended DLVO (DLVO−AB) model describes the interactions of smooth particles with solid surfaces above separation distances of 2 nm. According to this concept, cells adhere as they approach a surface close enough to be attracted and to be pulled into a sufficiently deep energy minimum. However, the DLVO−AB model often failed to describe bacterial adhesion. The most probable cause is the presence of bacterial surface polymers, which interfere with the DLVO−AB interactions. It has been postulated that polymers hinder the cells to reach the energy minimum, since the approach to the surface requires their compression (*3*, *4*). Promotion of adhesion (*5*) may be explained by polymer adsorption to surfaces. Polymers that are long enough to bridge the distance between cells and the surface may cause adhesion even when the cells do not experience DLVO−AB attraction. Such polymer-mediated adhesion may be irreversible (*1*, *4*−*7*). The assumption that polymer repulsion arises from the (physical) volume reduction of the cell envelope, whereas polymer attraction results from (chemical) adsorption of the polymers, implies that both polymer interactions may be almost independent of each other. Here we attempt (i) to quantify polymer interactions from the deviation of bacterial adhesion from DLVO−AB-based expectations and (ii) to calculate independently polymer attraction and repulsion between Gram-negative bacteria and glass. Results presented indicate that bacterial adhesion may be dominated by polymer interactions, which in the case of the lipopolysaccharides (LPS) of Gram-negative bacteria may protrude 30 nm or more from the outer cell membranes into the medium (*8*−*11*).

Theory

Bacterial Characteristics. Data on the bacterial strains *Stenotrophomonas maltophilia* DSM 50170 (*12*), *Stenotrophomonas maltophilia* 70401 (*13*), *Citrobacter freundii* PCM 1487 (*14*), *Escherichia coli* 08 DSM 46243 (*15*), *Escherichia coli* 07 DSM 46242 (*16*), and *Pseudomonas syringae* pv. *morsprunorum* C28 (*17*) were used. Relevant properties taken from published material (*18*−*20*) and additional data of *S. maltophilia* 70401 are summarized in Table 1. It has been shown that only 0.5% of the LPS of *S. maltophilia* 50170 had a long O antigen chain (ca. 30 nm), whereas the chains of the other LPS were short (ca. 1 nm) (*18*). The O antigens of each of the other bacteria were uniform in length. The strains can be divided into three groups according to their adhesion efficiency α_0 (*21*, *22*), i.e., the fraction of cells adhering upon contacting a surface (Table 2). *S. maltophilia* 50170 had a high α_0 (group 1), *C. freundii* and *S. maltophilia* 70401 had an intermediate α_0 (group 2), and *P. syringae* and both *E. coli* strains did not adhere to glass ($\alpha_0 \approx 0$; group 3). The LPS aggregated in water to micelles; those of *S. maltophilia* 50170 aggregated to vesicles (*18*). LPS adsorption on SiO_2 particles was characterized by the affinity (A), which is the product of the maximal surface coverage Γ_{max} and the equilibrium adsorption constant K_{ads} (*18*) (Table 2). Table 2 also gives the reversibility of bacterial adhesion and LPS adsorption upon drastic reduction of I. Adhesion of *S. maltophilia* strains and the LPS of group 2 could not be reverted. Adhesion by DLVO−AB interactions only should have been reverted since reduction of I diminishes DLVO−AB attraction. Therefore, irreversibility was indicative of polymer adsorption, which is less affected by changes of I. The adsorption of O antigens on SiO_2 could not be quantified in batch experiments but was detected by infrared spectroscopy (*19*). This showed that the adsorbed concentrations were only slightly below the detection limits of batch adsorption experiments given in Table 2.

* Corresponding author phone: 41 1 823 5519; fax: 41 1 823 5028; e-mail: harms@eawag.ch.

S0013-936X(98)00211-9 CCC: $15.00
Published on Web 08/12/1998

TABLE 1. Characteristics of Bacteria, LPS Micelles, and O Antigens

	cells			LPS micelles		O antigens	
strain	ζ potential[a] (mV)	contact angle (deg)	a_p (μm)	ζ potential[a] (mV)	a_p (nm)	MW (Da)	l_{Oanti}[b] (nm)
S. maltophilia 50170	-8.2 ± 1.1[c,d]	34 ± 3[d]	0.53[d]	-9.8 ± 1.7[d]	171 ± 90[d]	20 000[d]	30
S. maltophilia 70401	-2.0 ± 0.8[e]	19 ± 2[e]	0.56[e]	-9.3 ± 1.5	46 ± 21	38 500[f]	41
C. freundii	-30.0 ± 2.7[d]	27 ± 3[d]	0.46[d]	-11.0 ± 2.6[d]	50 ± 22[d]	19 600[d]	31
E. coli 08	-25.6 ± 1.0[d]	36 ± 2[d]	0.31[d]	-23.6 ± 1.2[d]	46 ± 20[d]	12 600[d]	22
E. coli 07	-44.8 ± 1.3[d]	29 ± 2[d]	0.52[d]	-7.4 ± 1.3[d]	29 ± 7[d]	21 600[d]	24
P. syringae	-5.0 ± 0.2[d]	21 ± 1[d]	0.50[d]	-7.7 ± 1.8[d]	32 ± 8[d]	24 000[d]	27

[a] ζ potentials in 0.1 M KCl (*20*). [b] Inferred from MW, repeating unit structure, and a_p of the micelles (*18*). [c] Standard deviation. [d] Values taken from ref *18*. [e] Values taken from ref *20*. [f] Values taken from ref *19*.

TABLE 2. Adhesion of Bacteria on Glass and Adsorption of LPS and O Antigens on SiO_2

	cells				LPS			O antigens		
	adhesion efficiency, α_0									
strain	0.1 M	0.01 M	0.001 M	reversibility[a] (%) at 0.1 M	A (mL mg^{-1})	K_{ads} (mL mg^{-1})	reversibility[a] (%)	Γ_{max} (mg m^{-2})	G^0_{ads} (kT/PS)	group
S. maltophilia 50170	0.55[b]	0.65[b]	0.51[b]	14[b]	4.8[b]	1.2[b]	91.5 ± 11.1[b]	nd	nd	1
S. maltophilia 70401	0.16[c]	0.26[c]	0.48[c]	18	33.0	15.9	57.3 ± 7.0	<0.055[d]	<-10.6	2
C. freundii	0.09[b]	0.02[b]	0.01[b]	74[b]	20.3[b]	3.5[b]	27.6 ± 4.6[b]	<0.037[d]	<-9.7	2
E. coli 08	0.007[b]	<0.005[b]	<0.005[b]	nd[e]	8.3[b]	5.9[b]	98.8 ± 12.8[b]	<0.035[d]	<-9.4	3
E. coli 07	0.02[b]	<0.005[b]	<0.005[b]	nd	4.9[b]	1.2[b]	78.8 ± 6.9[b]	nd	nd	3
P. syringae	0.02[b]	<0.005[b]	<0.005[b]	nd	3.3[b]	2.0[b]	83.9 ± 4.9[b]	nd	nd	3

[a] Reversibility upon lowering the ionic strength from 0.1 M to deionized water. [b] Values taken from ref *18* (LPS). [c] Values taken from ref *20*. [d] Values taken from ref *19*. [e] nd means not determined.

Approach. We attempted to calculate attractive and repulsive polymer contributions to bacterial adhesion as functions of the separation distance h to allow their additive combination with DLVO−AB interactions. Toward this end, we assumed that the Gibbs free enthalpy of bacterial adhesion $G^{tot}(h)$ is the sum of the DLVO−AB interaction enthalpy $G^{DLVO-AB}(h)$ and of the repulsive $G^{rep}(h)$ and attractive $G^{att}(h)$ polymer interaction enthalpies:

$$G^{tot}(h) = G^{DLVO-AB}(h) + G^{rep}(h) + G^{att}(h) \qquad (1)$$

It was furthermore assumed that the polymer interactions reach out from the same shell of the cell envelope as the DLVO−AB interactions. On the basis of these assumptions, polymer interactions can be inferred from the deviation of adhesion and adsorption data from DLVO−AB-based predictions. These experimentally inferred polymer interaction enthalpies were compared with independently calculated polymer interaction enthalpies.

Location of the Reference Shell for Distance-Dependent Interactions. DLVO−AB interactions were calculated according to Rutter and Vincent (*1*) and van Oss (*2*). Polymers can only interfere with DLVO−AB interactions when they project from the reference shell used for DLVO−AB calculations. This is because DLVO−AB interactions do not allow for contact between hydrophilic bacteria and SiO_2, but polymer adsorption and polymer compression require close contact between polymers and the surface. Hence, the DLVO−AB-relevant cell surface is located inside the outermost parts of the cell. We assumed that this reference shell is located at the basis of the O antigens and that the thickness of the polymer interaction layer is equal to the length of the O antigens l_{Oanti} (Table 1). The radius $a_p - l_{Oanti}$ was used for the DLVO−AB calculations.

Inference of Polymer Interactions from the Deviation of Adhesion/Adsorption Data from DLVO−AB Calculations. We inferred the depths of the energy minima G^{sm}_{exp} from adsorption and adhesion experiments and compared them with the depths of calculated DLVO−AB energy curves $G^{sm}_{DLVO-AB}$ (*23*). The contribution of polymer interactions G^{sm}_{pi} was then

$$G^{sm}_{pi} = G^{sm}_{exp} - G^{sm}_{DLVO-AB} \qquad (2)$$

For bacteria, G^{sm}_{exp} is proportional to α_0 (*23*). To calibrate the proportionality, we assumed that polymer repulsion was absent for the O antigen deficient *S. maltophilia* 50170 as discussed in ref 18, i.e., $G^{sm}_{exp} = G^{sm}_{DLVO-AB}$. For LPS micelles, G^{sm}_{exp} was inferred from K_{ads} as $G^{sm}_{exp} = -\ln(K_{ads})$ (*24*, *25*).

Calculation of Polymer Attraction. We had shown earlier that hydroxyl groups of O antigens of Gram-negative bacteria formed hydrogen bonds with surface hydroxyl groups of SiO_2 and surface-bound water (*19*). Formation of hydrogen bonds released on average an adsorption enthalpy G^0_{ads} of -9 kT per O antigen molecule, regardless of the type of O antigen (*19*). The attractive enthalpy G^{att}(h) is the product of G^0_{ads} and the number of adsorbed O antigens at $h < l_{Oanti}$:

$$G^{att}(h) = G^0_{ads}\Gamma_{max}\frac{N_A}{MW}F(h) \qquad (3)$$

with

$$F(h) = \pi(a_p^2 - [a_p - l_{Oanti} + h]^2) \qquad (4)$$

where N_A is Avogadro's number and MW is the molecular weight of the O antigens. Γ_{max} can be taken as the amount of adsorbed O antigens, since bacterial adhesion exposes the solid surface to saturating O antigen concentrations. $F(h)$ is the area of the flattened region that arises from the deformation of the polymer layer upon close contact with the solid surface.

Calculation of Polymer Repulsion. Polymer repulsion at $h < l_{Oanti}$ reflects entropic (elastic) and enthalpic (osmotic) energies:

$$G^{rep} = H^{rep} - TS^{rep} \qquad (5)$$

where H^{rep} is the change in enthalpy and S^{rep} is the change in entropy (*26*). S^{rep}, which arises from bending of polymers upon compression, was negligible for our system. H^{rep} represents the resistance of the polymer layer against water extrusion upon compression as was observed for the interaction of humic acid-covered latex particles with quartz (*27*). According to Amirbahman et al. and Penrod et al. (*26*, *28*), it is given by

$$H^{rep}(h) = \frac{2\pi\Phi^2 N_A(a_p - l_{Oanti})}{\bar{V}_l}(1/2 - \chi)(l_{Oanti} - h)^2\, kT \quad (6)$$

where Φ is the volume fraction of O antigens in the polymer interaction layer, V_l is the molar volume of water, and χ is the Flory−Huggins solvency parameter, which accounts for the affinity of the O antigens for water. In aqueous solutions, χ is generally in the range of 0.45−0.5 (*29*). For the O antigens, we took a value of 0.47 on the basis of data for several polysaccharides (*30*). The authors are aware of the fact that the choice of one value of χ does neglect the heterogeneity of the lipopolysaccharide chains. Φ is given by

$$\Phi = \frac{m_{Oanti}}{V_{pil}\rho} \quad (7)$$

where ρ is the polymer density in solution, which we calculated from the volume of water-dissolved dextran (ρ = 1.5 g cm^{-3}) (*31*). m_{Oanti} is the mass of O antigens, and V_{pil} is the volume of the polymer interaction layer with a thickness l_{Oanti}. m_{Oanti} was calculated from the molecular weight (MW) of the O antigens and the number of O antigens (N_{LPS}) per square meter of the reference shell. N_{LPS} of *E. coli* of 5.8 × 10^{17} m^{-2} (*32*) corresponds to the theoretical packing density of a simulated LPS structure (*33*). The area fraction of the reference shell that is occupied by long-chain O antigens f_{Oanti} is reduced by the contents of protein and short-chain LPS. Therefore,

$$m_{Oanti} = S\frac{N_{LPS} f_{Oanti} MW}{N_A} \quad (8)$$

where S is the surface area of the reference shell:

$$S = 4\pi(a_p - l_{Oanti})^2 \quad (9)$$

The volume of the polymer interaction layer V_{pil} is

$$V_{pil} = \frac{4}{3}\pi(a_p^3 - (a_p - l_{Oanti})^3) \quad (10)$$

LPS preparations contained negligible impurities of protein, i.e., $f_{Oanti} \approx 1$. For *S. maltophilia* 50170, $f_{Oanti} = 0.005$.

Results

DLVO−AB Curves. DLVO−AB energy curves were calculated for bacteria and glass beads (Figure 1) and for the corresponding LPS and SiO_2 powder (Figure 2). For bacteria and glass in 0.1 M KCl, $G^{sm}_{DLVO-AB}$ ranged from −11 to −22 kT at 5−6 nm from the surface. This would result in inactivated ($\alpha_0 \approx 1$) but reversible (upon reduction of I) adhesion. LPS were less attracted with $G^{sm}_{DLVO-AB}$ between −0.5 and −1.0 kT at 6 nm from the surface, except for *S. maltophilia* 50170, where $G^{sm}_{DLVO-AB}$ was −2.9 kT. The reach of the attraction was 10 nm. This would result in reversible low affinity adsorption.

Inference of Polymer Interactions from the Deviation of Adhesion/Adsorption Data from DLVO−AB Calculations. Weak adhesion of group 2 bacteria indicated G^{sm}_{exp} between −6.1 and −3.4 kT (Table 3). This is in agreement with a postulated minimum around −5 kT needed for adhesion (*1*, *7*, *34*). For all group 3 bacteria, G^{sm}_{exp} was shallower than −1 kT and, thus, insufficient to withstand the Brownian kinetic energy of bacteria of +1.5 kT (*35*). Deviations from $G^{sm}_{DLVO-AB}$ indicated repulsive G^{sm}_{p} between +11 and +19 kT for groups 2 and 3 bacteria. The efficient adsorption of LPS of groups 2 and 3 with G^{sm}_{exp} between −15.3 and −17.4 kT resulted in attractive G^{sm}_{pi} between −14.3 and −16.5 kT.

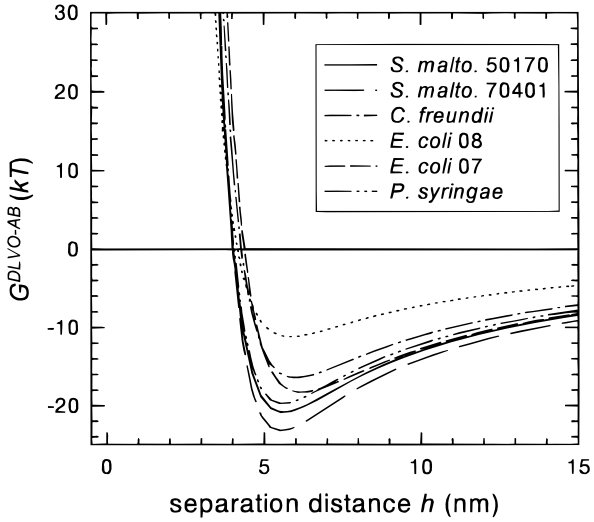

FIGURE 1. DLVO−AB interaction curves for bacteria and glass at I = 0.1 M.

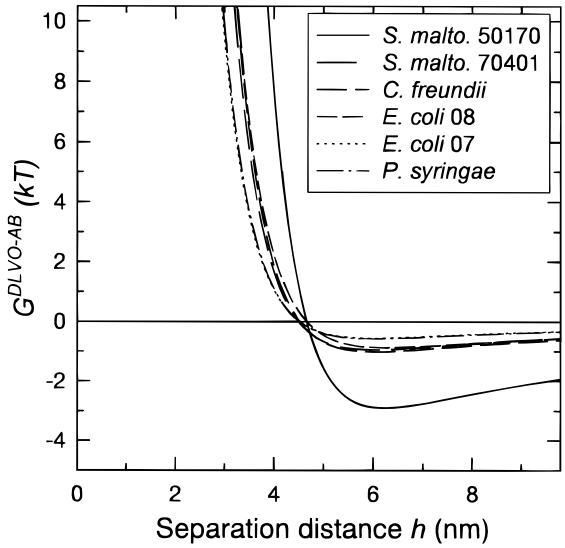

FIGURE 2. DLVO−AB interaction curves for LPS micelles and SiO_2 at I = 0.1 M.

Calculation of Total Interaction Energy Profiles. Polymer interactions of *S. maltophilia* 50170 were calculated for f_{Oanti} = 0.005, corresponding to Φ = 0.002. For each of the other bacteria we used estimates of f_{Oanti} of 0.3, 0.72, and 0.90, resulting in Φ values of 0.15, 0.30, and 0.35, respectively. Γ_{max} was varied within 1 order of magnitude below the detection limits of adsorption experiments given in Table 2. Figures 3−5 show the total interaction energy profiles including DLVO−AB and polymer interactions for *S. maltophilia* 50170, *C. freundii*, and *E. coli* 08, which are representative for the three groups of bacteria.

For *S. maltophilia* 50170, total energy calculations were in agreement with its efficient irreversible adhesion (Figure 3). Polymer repulsion was small, and polymer and DLVO−AB attraction added to a $G^{sm}_{tot} \leq -80$ kT even at the lowest value of Γ_{max}. For the clarity, the individual G^{att} curves that

TABLE 3. Strength of Polymer Interactions

	bacteria			LPS		
	$G^{sm}_{DLVO-AB}$ (kT)	G^{sm}_{exp} (kT)	G^{sm}_{pi}[a] (kT)	$G^{sm}_{DLVO-AB}$ (kT)	G^{sm}_{exp} (kT)	G^{sm}_{pi} (kT)[a]
S. maltophilia 50170	−20.8	−20.8	0	−2.9	−9.3	−6.4
S. maltophilia 70401	−23.2	−6.1	+17.1	−0.9	−17.4	−16.5
C. freundii	−16.4	−3.4	+13.0	−1.0	−15.3	−14.3
E. coli 08	−11.2	−0.3	+10.9	−0.9	−16.4	−15.5
E. coli 07	−18.3	−0.8	+17.5	−0.5	−15.3	−14.8
P. syringae	−19.7	−0.8	+18.9	−0.6	−15.5	−15.0

[a] $G^{sm}_{pi} = G^{sm}_{exp} - G^{sm}_{DLVO-AB}$.

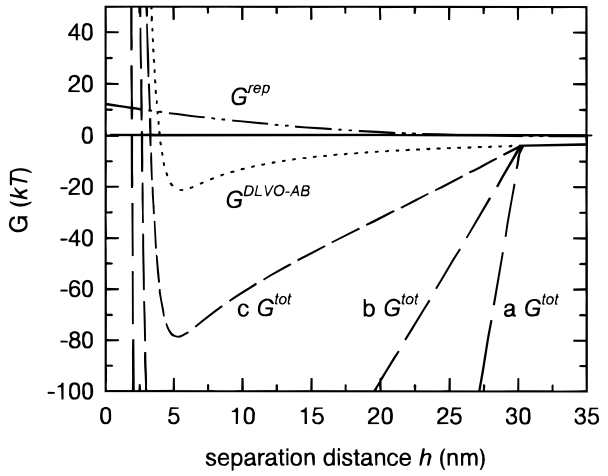

FIGURE 3. Total interaction energy curves for *S. maltophilia* 50170 and glass at $I = 0.1$ M. Γ_{max} was 0.035 (a), 0.010 (b), and 0.003 mg m^{-2} (c).

result from the variation of Γ_{max} are not shown. The strong polymer attraction was in agreement with the irreversibility of the adhesion observed with whole cells.

Energy calculations for *C. freundii* corresponded to its weak reversible adhesion (Figure 4A). Strong polymer repulsion caused a drastically outward-shifted energy minimum at ca. 30 nm from the surface. Individual G^{rep} curves for different f_{Oanti} are not shown. Assuming $f_{Oanti} = 0.72$ (Figure 4A, curve b), as reported for *Salmonella typhimurium* (*36*), and Γ_{max} equal to the detection limit of batch sorption experiments, polymer repulsion hindered the cells to approach the glass further than $h \approx l_{Oanti}$. G^{sm}_{tot} at this separation distance matched the experimental value of −3.4 kT (Table 3) and was almost exclusively determined by the DLVO−AB attraction. This is in agreement with the detachment of *C. freundii* when the DLVO−AB attraction was diminished by reducing *I*. Higher values for f_{Oanti} (0.9 in curve a) had little additional effect on the repulsion. For polymer attraction to become dominant, unrealistically low value of f_{Oanti} (0.3 in curve c) for this strain would be needed. Γ_{max} was varied over 2 orders of magnitude (Figure 4B). Curves b and c show that polymer repulsion dominated over the range of likely values for Γ_{max}. Much stronger adsorption has been observed with O antigens and either Al_2O_3 or TiO_2 (*19*). To illustrate the effect of strong adsorption, we calculated the energy for Γ_{max} as was measured with Al_2O_3. In this case, polymer attraction became dominant (curve a).

Energy calculations for group 3 bacteria (Figure 5) were similar to those for group 2 and did not correspond with the absence of adhesion. G^{sm}_{tot} of ca. −5 kT was considerably deeper than the experimental observation of −0.3 kT and would have allowed for reversible adhesion. Total energy calculations for LPS micelles and vesicles corresponded to the observed LPS adsorption. Φ of the LPS micelles and vesicles of groups 2 and 3 ranged between 0.019 and 0.097,

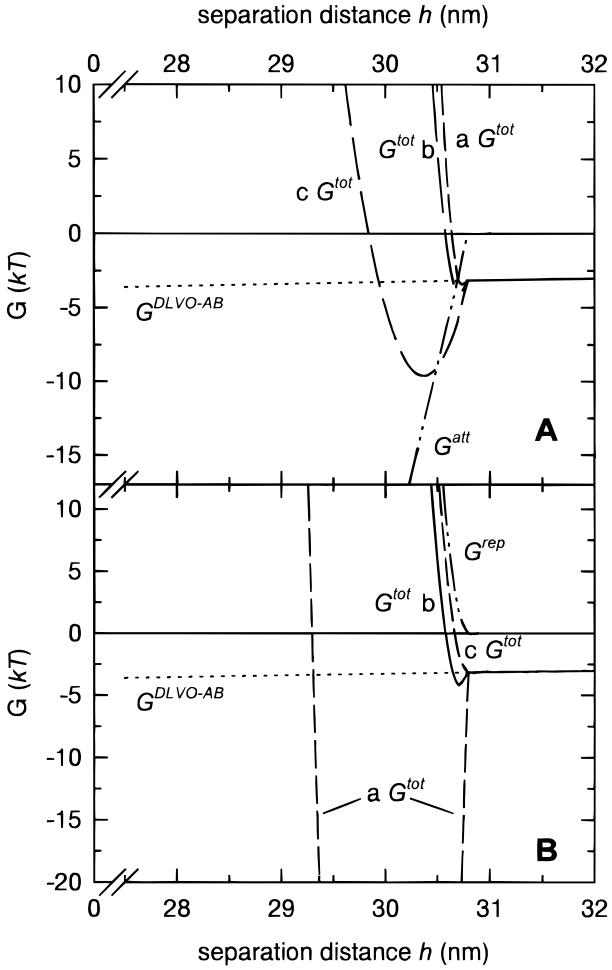

FIGURE 4. Total interaction energy curves for *C. freundii* and glass at $I = 0.1$ M. In panel A, f_{Oanti} was 0.90 (a), 0.72 (b), and 0.3 (c) with $\Gamma_{max} = 0.037$ mg m^{-2}. In panel B, Γ_{max} was 0.30 (a), 0.037 (b), and 0.003 mg m^{-2} (c) with $f_{Oanti} = 0.72$.

while Φ for the LPS of the group 1 bacterium was 0.0017. As an example, results for *C. freundii* LPS are shown (Figure 6). Since DLVO−AB interactions were low, polymer interactions fully dominated LPS adsorption. The loose packing of the outer part of the polysaccharide layer, caused by the sharp curvature of LPS micelles, resulted in weak polymer repulsion and facilitated close contact of polysaccharides with the solid. It may, at higher values of Γ_{max}, have resulted in the observed strong irreversible polymer attraction.

Discussion

We proposed a method to calculate polymer interactions between bacteria and solid surfaces in a distance-dependent manner and combined them in an additive manner with the DLVO−AB model. Calculations assume that polymer repul-

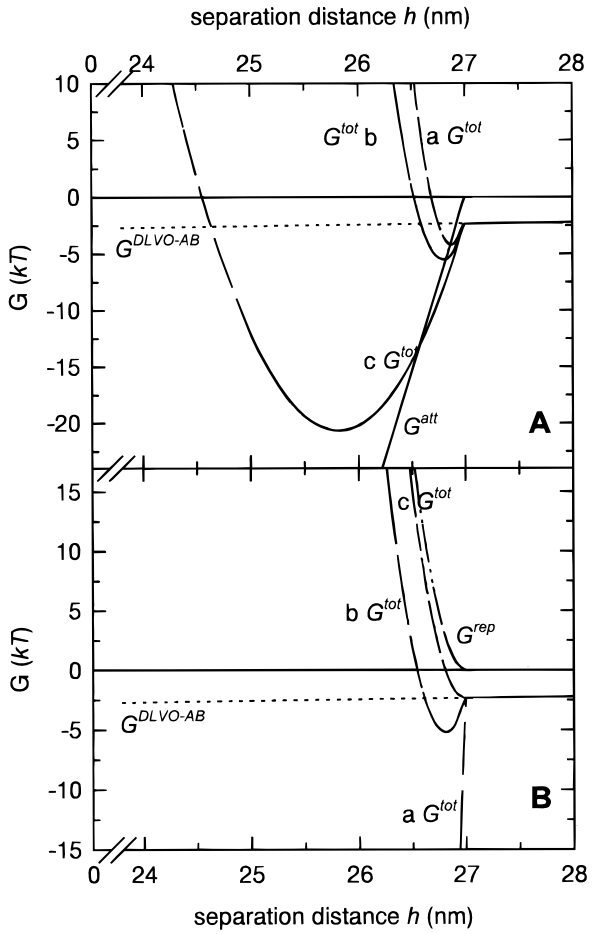

FIGURE 5. Total interaction energy curves for *E. coli* 08 and glass at $I = 0.1$ M. In panel A, f_{Oanti} was 0.90 (a), 0.72 (b), and 0.03 (c) with $\Gamma_{max} = 0.035$ mg m^{-2}. In panel B, Γ_{max} was 0.3 (a), 0.035 (b), and 0.003 mg m^{-2} (c) with $f_{Oanti} = 0.72$.

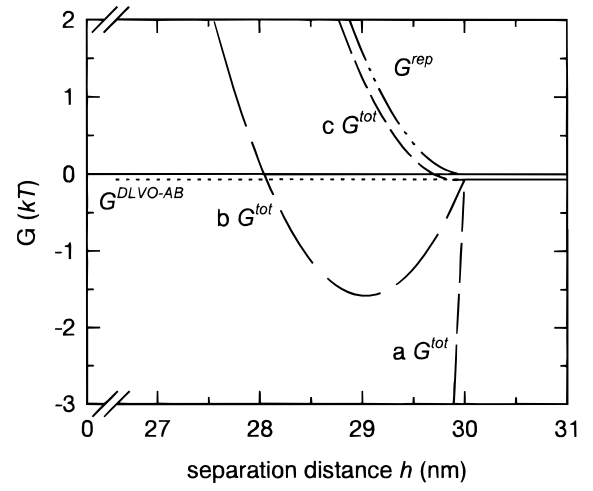

FIGURE 6. Total interaction energy curves for the LPS of *C. freundii* and SiO_2 at $I = 0.1$ M. Γ_{max} was 0.30 (a), 0.035 (b), and 0.003 mg m^{-2} (c).

sion arises when cell envelopes are compressed, whereas polymer attraction reflects adsorption of polymers to the solid surface. The calculation of polymer interactions is limited by their sensitivity to poorly accessible physical and chemical properties of bacterial envelopes. Moreover, our model relies on the hardly verifiable (and hardly refutable) assumption of a common reference shell from which all interactions arise. At the present, the reference shells of the individual forces cannot be defined, and we renounced to use them as additional fitting parameters. Obviously, any observation could be matched in a fitting routine involving five individual forces with different decay functions. Good agreement with experimental observations, nevertheless, indicates that the assumptions of polymer compression and adsorption are fulfilled and that our approach may help to overcome shortcomings of the DLVO−AB concept, e.g., its negligence of the frequently observed irreversibility of bacterial adhesion.

Polymer Repulsion. The assumption was tested that denser packing of O antigens in the cell envelope results in higher resistance against compression and in lower adhesion (Figures 4A and 5A). The integrity of the outer membrane relies on a relatively fixed packing density of LPS in the lipid bilayer. Therefore, the packing density of the outward-directed polysaccharide layer depends on (i) the area fraction of the lipid bilayer that is occupied by LPS rather than by outer membrane proteins, (ii) on the uniformity in length of the O antigens, and (iii) on the curvature of the lipid bilayer. The curvature simply reflects the cell radius, whereas uncertainty about LPS uniformity and outer membrane protein contents is the main impediment of a straightforward calculation of polymer repulsion. It seems that, for example, the presence of a small fraction of slightly longer O antigens could shift the overall polymer interaction from repulsive to attractive. Our calculations show that the low adhesion of group 2 bacteria (Figure 4A) may result from uniform LPS in combination with outer membrane protein contents such as reported for *S. typhimurium* (*36*). The accessible depth of the DLVO−AB interactions above the critical separation distance at which further approach is prevented may determine the adhesion efficiency of these bacteria. Group 3 bacteria did not adhere on glass, indicating that G^{sm}_{exp} was below −1 kT (Table 3). The reason for this discrepancy with a calculated energy minimum at $h \approx l_{Oanti}$ of −5.0 kT remains unclear. The calculated minimum is determined by DLVO−AB and by polymer interactions. Therefore, inadequate parameters used for DLVO−AB calculations and/or an underestimation of f_{Oanti} and/or an overestimation of Γ_{max} could be responsible for the discrepancy. The packing density of O antigens in the cell envelope of *S. maltophilia* 50170 is small and probably results in much better compressibility. These bacteria may approach the solid up to the secondary minimum of the DLVO−AB interactions (Figure 3) as is supported by the high adhesion efficiency of this strain. Reduced polymer repulsion of LPS micelles (Figure 6) results from the strong curvature of the lipid bilayer, causing loose packing of the tips of the O antigens. The better adhesion of LPS micelles as compared to the corresponding bacteria indicates the actual influence of f_{Oanti}.

Polymer Attraction. Polymer attraction was assumed to depend on Γ_{max} (Figures 3, 4B, and 5B). This is because nearby bacteria or micelles cause very high polysaccharide concentrations near the solid. Even the few O antigens of *S. maltophilia* 50170 were assumed sufficient for surface saturation. The maximum coverage of SiO_2 was generally low (Table 2), as was the overall effect of polymer attraction for five out of six bacteria. At realistic Γ_{max} values, only 1−10% of the O antigens in contact with the surface are actually adsorbed. These are reasonable percentages since adsorption of more O antigens by hydrogen bonding would cause irreversible adhesion. The reversible adhesion of *C. freundii* and other bacteria (*3*) upon lowering I, however, indicates that polymer attraction is lower than the sum of electrostatic repulsion at low I and polymer repulsion. Other bacterial surface polymers, e.g., hydrophobic proteins ($\Gamma_{max} \approx 1$ mg m^{-2}; $G^0_{ads} \approx -16$ kT) sorb better to glass and may cause dominant polymer attraction (*37*−*39*). Cell surface proteins also affect the hydrophobicity of bacteria and result in

increased acid−base (hydrophobic) attraction (*2*). Accordingly, Gram-positive bacteria with protein coatings adhered efficiently (*3*). Irreversible adhesion of *S. maltophilia* 50170 (Table 2) shows that polymer attraction may overcome electrostatic repulsion at low ionic strength.

Predictability of Bacterial Adhesion and Subsurface Transport. We postulate that the interplay of polymer compressibility and affinity for the solid determines whether polymers favor or inhibit adhesion. In case of *S. maltophilia* 50170, DLVO−AB attraction and polymer adsorption overcompensated weak polymer repulsion. For five of the six bacteria, polymer repulsion appeared to exceed DLVO−AB attraction and polysaccharide adsorption. This shows that attractive DLVO−AB interaction forces do not necessarily lead to bacterial adhesion. Since polymer interactions may dominate the interaction of bacteria with solids, prediction of bacterial mobility in the subsurface requires detailed information about the cell surface architecture in addition to the classical characterization of bacterial surface charge and contact angles. At the present, it is uncertain, whether bacteria can be characterized rigorously enough for a priori prediction of adhesion. Results with group 3 bacteria indicate that filtration of bacteria by materials such as SiO_2 may be negligible and may allow the long-distance transport of bacteria. This may account for the observed displacement of bacteria in fast-flowing groundwater of up to 920 m as reviewed by Gerba (*40*). Similar transport distances can be extrapolated from a recent study conducted at slow flow rate in quartz sand, where the adhesion efficiency of a subpopulation of *Pseudomonas* sp. B13 appeared to be close to zero (*41*). In the present study, the enteric organisms *E. coli* 08 and *E. coli* 07 were among those organisms interacting least with SiO_2. These findings do not necessarily challenge present standards for bacteriological drinking water safety. However, the possible existence of nonfilterable organisms should be considered.

Acknowledgments

We thank A. Amirbahman for his help with the calculation of polymer repulsion and J. C. Westall for valuable comments on the manuscript.

Glossary

A	affinity (L m^{-2})
a_p	radius of bacteria or LPS micelles (m)
$F(h)$	area of contact plane (m^2)
f_{Oanti}	area fraction of the reference shell occupied by long O antigens
$G^{att}(h)$	attractive polymer interaction energy (kT)
$G^{DLVO-AB}(h)$	DLVO−AB interaction energy (kT)
$G^{rep}(h)$	repulsive polymer interaction energy (kT)
$G^{sm}_{DLVO-AB}$	depth of DLVO−AB secondary minimum (kT)
G^{sm}_{exp}	experimentally observed depth of secondary minimum (kT)
G^{sm}_{pi}	polymer interaction energy at total energy minimum (kT)
G^{sm}	depth of total energy minimum (kT)
$G^{tot}(h)$	total interaction energy (kT)
G^0_{ads}	adsorption enthalpy (kT)
h	separation distance (m)
H^{rep}	repulsive enthalpy change (kT)
I	ionic strength (M)
K_{ads}	adsorption equilibrium constant (L g^{-1})
k	Boltzmann constant (J K^{-1})
l_{Oanti}	length of O antigens (m)
MW	molecular weight of O antigens (g mol^{-1})
m_{Oanti}	O antigen mass in the polymer interaction layer (g)
N_A	Avogadro's number (mol^{-1})
N_{LPS}	number of LPS per square meter (m^{-2})
S_{mic}	surface area of the reference shell (m^2)
S_{rep}	repulsive entropy change (kT)
T	temperature (K)
$\bar{V}_l$	molar volume of the solvent (m^3 mol^{-1})
V_{pil}	volume of the polymer interaction layer (m^3)
α_0	adhesion efficiency
Γ_{max}	maximal surface coverage with O antigens (g m^{-2})
ρ	polymer density (g m^{-3})
Φ	polymer volume fraction
χ	Flory−Huggins solvency parameter

Literature Cited

(1) Rutter, P. R.; Vincent, B. In *Microbial adhesion to surfaces*; Berkeley, R. C. W., Lynch, R. M., Melling, J., Rutter, P. R., Vincent, B., Eds.; Horwood: Chichester, 1980; pp 79−93.
(2) van Oss, C. J., Ed. *Interfacial forces in aqueous media*; Marcel Dekker: New York, 1994.
(3) Rijnaarts, H. H. M.; Norde, W.; Bouwer, E. J.; Lyklema, J.; Zehnder, A. J. B. *Environ. Sci. Technol.* **1996**, *30*, 2877−2883.
(4) Van Loosdrecht, M. C. M.; Lyklema, J.; Norde, W.; Zehnder, A. J. B. *Microbiol. Rev.* **1990**, *54*, 75−87.
(5) Marshall, K. C.; Stout, R.; Mitchell, R. *J. Gen. Microbiol.* **1971**, *68*, 337−348.
(6) Neu, T. R.; Marshall, K. C. *J. Biomater. Appl.* **1990**, *5*, 107−133.
(7) Rijnaarts, H. H. M.; Norde, W.; Bouwer, E. J.; Lyklema, J.; Zehnder, A. J. B. *Appl. Environ. Microbiol.* **1993**, *59*, 3255−3265.
(8) Arredondo, R.; Garcia, A. J. C. A. *Appl. Environ. Microbiol.* **1994**, *60*, 2846−2851.
(9) Palomar, J.; Leranoz, A. M.; Vinas, M. *Microbios* **1995**, *81*, 107−113.
(10) Paradis, S.-E.; Dubreuil, D.; Rioux, S.; Gottschalk, M.; Jacques, M. *Infect. Immun.* **1994**, *62*, 331−3319.
(11) Williams, V.; Fletcher, M. *Appl. Environ. Microbiol.* **1996**, *62*, 100−104.
(12) Neal, D. J.; Wilkinson, S. G. *Carbohydr. Res.* **1979**, *69*, 191−201.
(13) Winn, A. M.; Galbraith, L.; Temple, G. S.; Wilkinson, S. G. *Carbohydr. Res.* **1993**, *247*, 249−254.
(14) Gamian, A.; Romanowska, E.; Romanowska, A.; Lugowski, C.; Dabrowski, J.; Trauner, K. *Eur. J. Biochem.* **1985**, *146*, 641−647.
(15) Jansson, P.-E.; Lönnegren, J.; Widmalm, G.; Leontein, K.; Slettengren, K.; Tiller, P. T.; Svenson, S. B.; Wrangsell, G.; Dell, A. *Carbohydr. Res.* **1985**, *145*, 59−66.
(16) L'Vov, V. L.; Shashkov, A. D. B. A.; Kochetkov, N. K.; Jann, B.; Jann, K. *Carbohydr. Res.* **1984**, *126*, 249−259.
(17) Smith, A. R. W.; Zamze, S. E.; Munro, S. M.; Carter, K. J.; Hignett, R. C. *Eur. J. Biochem.* **1985**, *149*, 73−78.
(18) Jucker, B. A.; Harms, H.; Zehnder, A. J. B. *Colloids Surf. B* **1998**, *11*, 33−45.
(19) Jucker, B. A.; Harms, H.; Hug, S.; Zehnder, A. J. B. *Colloids Surf. B* **1997**, *9*, 331−343.
(20) Jucker, B. A.; Harms, H.; Zehnder, A. J. B. *J. Bacteriol.* **1996**, *178*, 5472−5479.
(21) Elimelech, M.; O'Melia, C. R. *Environ. Sci. Technol.* **1990**, *24*, 1528−1536.
(22) Rijnaarts, H. H. M.; Norde, W.; Bouwer, E. J.; Lyklema, J.; Zehnder, A. J. B. *Environ. Sci. Technol.* **1996**, *30*, 2869−2876.
(23) Meinders, J. M.; Van der Mei, H. C.; Busscher, H. J. *J. Colloid Interface Sci.* **1995**, *176*, 329−341.
(24) Pradip, Y.; Attia, A.; Fürstenau, D. W. *Colloid Polym. Sci.* **1980**, *258*, 1343−1353.
(25) Stumm, W., Ed. *Chemistry of the solid-water interface*; John Wiley: New York, 1992.
(26) Amirbahman, A. Ph.D. Thesis, University of Irvine, Irvine, CA, 1993.

(27) Amirbahman, A.; Olson, T. M. *Environ. Sci. Technol.* **1993**, *27*, 2807−2813.
(28) Penrod, S. L.; Olson, T. M.; Grant, S. B. *Langmuir* **1996**, *12*, 5576−5587.
(29) Fleer, G. J.; Lyklema, J. In *Adsorption from Solution at the Solid/Liquid Interface*; Parfitt, G. D., Rochester, C. H., Eds.; Academic Press: London, 1983; p 420.
(30) Radosta, S.; Schierbaum, F.; Reuther, F.; Anger, H. *Strach/Stärke* **1989**, *41*, 395−401.
(31) Weast, R. C., Ed. *Handbook of chemistry and physics*; CRC Press: Boca Raton, FL, 1986−1987.
(32) DiRienzo, J. M.; Nakamura, K.; Masayori, I. *Annu. Rev. Microbiol.* **1978**, *47*, 481−532.
(33) Kastowsky, M.; Sabisch, A.; Gutberlet, T.; Bradaczek, H. *Eur. J. Biochem.* **1991**, *197*, 707−716.
(34) Van Loosdrecht, M. C. M.; Lyklema, J.; Norde, W.; Zehnder, A. J. B. *Microb. Ecol.* **1989**, *17*, 1−15.
(35) Calleja, G. B. *Colloids Surf. B* **1994**, *2*, 133−149.
(36) Nikaido, H.; Vaara, M. In *Escherichia coli and Salmonella typhimurium*; American Society for Microbiology: Washington, DC, 1983; p 3.
(37) Norde, W. *Cell Mater.* **1995**, *5*, 97−112.
(38) Duinhoven, S.; Poort, R.; Van der Voet, G.; Agterof, W. G. M.; Norde, W.; Lyklema, J. *J. Colloid Interface Sci.* **1995**, *170*, 340−350.
(39) Norde, W.; Lyklema, J. *Colloids Surf.* **1989**, *38*, 1−13.
(40) Gerba, C. P. In *Groundwater Pollution Microbiology*; Bitton, G., Gerba, C. P., Eds.; John Wiley: New York, 1984; pp 225−234.
(41) Simoni, S. F.; Harms, H.; Bosma, T. N.; Zehnder, A. J. B. *Environ. Sci. Technol.* **1998**, *32*, 2100−2105.

Received for review March 3, 1998. Revised manuscript received June 1, 1998. Accepted June 15, 1998.

ES980211S